

J. Natn. Sci. Foundation Sri Lanka 2002 30(3&4): 171-184

QUANTITATIVE STRUCTURE ACTIVITY RELATIONSHIPS FOR GUANIDINOTHIAZOLECARBOXAMIDES USING THEORETICALLY CALCULATED MOLECULAR DESCRIPTORS

SUSIL J. SILVA* and KAMALA S. JAYASUNDERA

Department of Chemistry, University of Sri Jayewardenepura, Gangodawila, Nugegoda

(Received: 20 November 2001 ; accepted: 06 August 2002)

Abstract: Guanidinothiazolecarboxamides (GTCs) are a class of anti-tumor agents supposed to exert their anti-tumor activity through intercalation. The intercalation of GTCs with DNA duplex tetramer d(GCTA) was investigated using molecular mechanics methods. The results showed that GTCs intercalate favourably at the CG/TA step. Two quantitative structure activity relationships (QSAR) for 5 and 6 substituted GTCs were obtained using theoretically calculated molecular descriptors.

Keywords: Anti-tumor activity, guanidinothiazolecarboxamides, molecular descriptors, molecular mechanics, quantitative structure activity relationship (QSAR) quantum mechanics

INTRODUCTION

Cancer is one of the most formidable diseases in the world. Lung cancer, in particular, has increased rapidly in incidence, due in part to the long-term effects of air pollution, especially that from tobacco. All structure-activity relationships made so far on anti-tumor drugs have primarily established that the main cellular target of these drugs is DNA. The anti-tumor drugs that directly bind with DNA and stop its proliferation mainly involve three types of binding¹: 1) covalent bond formation 2) intercalation and 3) non-intercalation groove binding.

Guanidinothiazolecarboxamides (GTCs), (Figure 1), are a novel class of anti-tumor agents found to be systemically active against experimental pulmonary metastases 3LL Lewis Lung Carcinoma.^{2,3} The GTCs are supposed to exert their anti-tumor effects through intercalation.¹ It has been generally observed that fused ring aromatic compounds bind most strongly to DNA as an intercalation complex.^{4,5} The widely studied intercalators are the derivatives of 9-anilinoacridine, 9-aminoacridine and the analogues of anthracycline.⁶ There are no detailed experimental or theoretical results available in literature on the favourable binding sites of GTCs to DNA. The major objectives of this research project are 1) to find favourable binding sites of GTC to DNA and 2) to explore whether there exists a correlation between biological activity of GTCs and their calculated electronic and structural properties. The concept of quantitative structure activity relationship (QSAR) is to transform searches for compounds with desired properties using chemical intuition and experience into a mathematically quantified and

* Corresponding author

computerised form. The importance of this later objective is that once a correlation between structure and activity is found, any number of compounds, including those not yet synthesized, can be readily screened on the computer in order to select structures with the desired properties. It is then possible to select the most promising compounds to synthesize and test in the laboratory.

To obtain a significant correlation, it is crucial that appropriate descriptors be employed, whether they are theoretical, empirical or derived from readily available experimental characteristics of the structure. Many descriptors reflect simple molecular properties and can thus provide insight into the physicochemical nature of the activity under consideration. Recent progress in computer hardware and the development of efficient algorithms have assisted the routine development of molecular quantum mechanical calculations. New semi-empirical methods supply realistic quantum chemical molecular properties in a relatively short computational time frame using even a personal computer. Quantum chemical calculations are thus an attractive source of new molecular descriptors, which can, in principle, express all of the electronic and geometric properties of molecules and their interactions. The quantum chemical descriptors have been correlated with biological activities such as enzyme inhibition activity, hallucinogenic activity, etc.⁷⁻¹⁰ In using theoretically based descriptors with a series of related compounds, the computational error is considered to be approximately constant throughout the series. A basic weakness of theoretical descriptors is the failure to directly address the bulk effects.¹¹

In this study, semi-empirical quantum chemical and molecular mechanics methods were used to obtain molecular descriptors of free drug molecules. The favourable intercalating sites for drug molecules were investigated by using the molecular mechanics methods.

METHODS AND MATERIALS

Computational Methods

Calculation of Molecular Descriptors: Initial atomic coordinates of all GTC molecules investigated in this study were obtained from the X-ray crystal structure of 5F-GTC.³ All structures were first energy minimised in the gas phase within molecular mechanics (MM) using the MMX force field¹⁷ and the resulting structures were further optimised by the semi-empirical quantum chemical method PM3. The calculations were performed using PCMODEL¹² and MOPAC version 5¹³ software packages. Finally, the gas phase optimised structures were re-optimised in the aqueous phase with the PM3 method using the AMSOL¹⁴ package. LogP (partition coefficient between octanol and water) was calculated by the Crippen's fragmentation¹⁶ using the CHEMDRAW¹⁸ program.

Intercalation of GTC with DNA: In order to determine the favourable intercalating site for GTC, three DNA base steps CG/TA, GC/CG and TA/AT were considered. GTC was intercalated using the PCMODEL software into DNA tetramer d(GCTA)₂ having the above base steps. The DNA tetramer was constructed using the X-ray crystal structure of d(CGCTAGCG)₂.¹⁵ The intercalated GTC-DNA complexes, DNA tetramer and GTCs were energy minimised using the MMX force field. The binding energy (BE) of the GTC-DNA complex was calculated using the following equation.

$$BE = E_{\text{GTC-DNA}} - E_{\text{DNA}} - E_{\text{DNA}}$$

where E_{DNA} is the energy of the DNA fragment, E_{GTC} is the energy of GTC and $E_{\text{GTC-DNA}}$ is the energy of the GTC-DNA complex.

Multiple linear regression analysis

A QSAR generally takes the form of a linear equation

$$\text{Biological Activity} = C_1P_1 + C_2P_2 + C_3P_3 + \dots + C_nP_n + \text{Constant}$$

Where the parameters P_1 through P_n are computed for each molecule in the series and coefficients C_1 through C_n are calculated by fitting variations in the parameters and the biological activity using multiple linear regressions.

RESULTS

The wireframe model of the energy minimised structure of 5F-GTC in the gas phase using the PM3 method is shown in Figure 1. The calculated gas phase and aqueous phase molecular properties of 5 and 6 substituted GTCs using the PM3 and MM methods are given in Tables 1 and 2 respectively. Energies of the HOMO (highest occupied molecular orbital) and LUMO (lowest unoccupied molecular orbital) are very popular quantum chemical descriptors. In Tables 1 and 2, the ionisation energy (IE) is calculated as the negative value of the energy of the HOMO. The polarity of a molecule is well known to be important for various physicochemical properties. The most obvious and most often used quantity to describe the polarity is the dipole moment of the molecule. The total dipole moment given in Tables 1 and 2, however, reflects only the global polarity of a molecule. Formation of an intra-molecular hydrogen bond between N19 and H29 atoms was observed in the PM3 optimised structures. The intra-molecular hydrogen bond distance, N19-H29 for 5 and 6 substituted GTCs is given in Table 1. Since the intra-molecular hydrogen bond stabilises the molecule, we have considered this hydrogen bond distance as a descriptor in QSAR analysis.

Table 1: Calculated gas phase molecular properties of 5 and 6-substituted GTCs

Substitute	HF ^a	IE ^b	E _{LUMO} ^c	DM ^d	BE ^e	N19-H29 ^f
H	77.501	8.8323	-1.14285	4.478	-20.427	2.301
6NO ₂	68.889	9.19877	-1.58966	9.29	-24.296	2.312
6Cl	71.127	8.81791	-1.19482	4.709	-25.251	1.981
6F	35.169	8.90049	-1.17719	5.528	-22.811	1.959
6CN	113.072	9.07093	-1.32352	6.96	-25.113	1.995
6CH ₃	68.158	8.71981	-1.12994	4.39	-23.897	2.3
6C(Me) ₃	54.564	8.75473	-1.13105	4.124	-27.541	1.975
6CH(Me) ₂	59.679	8.7606	-1.09833	4.63	-25.897	1.955
6(CH ₂) ₂ Me	58.367	8.72227	-1.12942	4.417	-27.189	2.3
6OCH ₃	40.695	8.82623	-1.07413	3.608	-22.711	2.292
6OCH ₂ Me	35.554	8.56368	-1.12076	5.207	-23.518	1.973
6O(CH ₂) ₃ Me	24.901	8.56608	-1.12116	5.187	-24.924	1.973
6SCH ₃	77.687	8.36986	-1.16525	6.039	-25.434	2.302
6CH ₂ CH ₃	63.656	8.76854	-1.13713	-	-	-
H	77.501	8.8323	-1.14285	4.478	-20.427	2.301
5F	34.943	8.92754	-1.17969	4.161	-22.562	1.961
5NO ₂	69.432	9.14921	-1.38451	5.914	-24.347	2.311
5OCHMe ₂	29.369	8.7678	-1.11614	5.294	-19.36	1.953
5Ph	101.884	8.74029	-1.15321	4.315	-15.187	1.976
5OH	33.219	8.79874	-1.10775	3.799	-27.949	1.959
5SCH ₃	78.513	8.506	-1.11925	3.423	-	-
5OCH ₂ Me	34.453	8.76	-1.11244	5.718	-	-

^a heat of formation in kcal, ^b ionisation energy in eV, ^c energy of lowest unoccupied molecular orbital in eV, ^d dipole moment in debye, ^e binding energy in kcal/mol, ^f intramolecular hydrogen bond distance between N19 and H29 in Å.

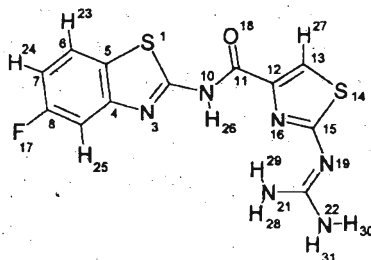


Figure 1: The gas phase energy minimised structure of 5F-GTC using the PM3 semi-empirical method.

Table 2: Calculated aqueous phase molecular properties of 5 and 6 substituted GTCs

Substitute	HF ^a	IE ^b	E _{LUMO} ^c	DM ^d	ΔG_p^e	ΔG_{cd}^f	ΔG^g
H	84.583	8.90395	-1.40843	9.168	-21.636	-7.925	-22.478
6NO ₂	80.052	8.6913	-1.96946	14.315	-27.24	-4.928	-21.005
6Cl	81.586	8.67251	-1.43132	10.985	-22.269	-8.064	-19.874
6F	43.243	8.85686	-1.48393	9.879	-23.724	-8.144	-23.794
6CN	124.399	8.67571	-1.56658	12.789	-25.608	-6.954	-21.235
6CH ₃	75.216	8.89917	-1.40201	9.066	-21.456	-7.601	-22
6C(Me) ₃	63.481	8.96722	-1.34862	9.953	-24.825	-7.742	-23.649
6CH(Me) ₂	67.984	8.96637	-1.35681	9.913	-24.883	-7.911	-24.489
6(CH ₂) ₂ Me	65.129	8.90093	-1.40379	9.148	-21.023	-7.177	-21.438
6OCH ₃	45.598	8.99654	-1.33209	9.56	-25.486	-9.471	-27.054
6OCH ₂ Me	47.877	8.62956	-1.31303	12.835	-26.347	-7.539	-21.563
6O(CH ₂) ₃ Me	36.769	8.65395	-1.32651	12.587	-25.48	-7.259	-20.871
6SCH ₃	90.052	8.66478	-1.51847	11.786	-24.089	-8.748	-20.472
H	84.583	8.904	-1.408	9.606	-21.636	-7.925	-22.478
5F	44.269	8.88025	-1.48413	10.01	-24.981	-8.179	-23.834
5NO ₂	80.162	8.69291	-1.66349	7.762	-26.572	-4.917	-20.759
5OCHMe ₂	38.185	8.92169	-1.38843	11.34	-25.406	-8.737	-25.328
5Ph	108.545	8.89206	-1.42395	9.248	-22.277	-8.236	-23.852
5OH	44.203	8.91	-1.364	10.291	-30.017	-11.18	-30.214
5SCH ₃	90.219	8.66464	-1.42156	10.213	-23.978	-8.749	-21.021
5OCH ₂ Me	43.319	8.89012	-1.3748	9.557	-26.378	-8.806	-26.318

^a heat of formation in kcal/mol; ^b ionisation energy in eV; ^c energy of lowest unoccupied molecular orbital in eV; ^d dipole moment in deby; ^e polarisation free energy of solvation in kcal/mol; ^f cavity-dispersion-solvent structure free energy in kcal/mol; ^g total free energy of solvation in kcal/mol

The binding energies for some 5 and 6 substituted GTCs intercalated into DNA tetramer d(GCTA)₂ are tabulated in Table 3. Among the three base pair steps (GC/CG, CG/TA and TA/AT) investigated in this study, the results showed that GTC intercalates more favourably at the CG/TA step. The energy minimised structures of the DNA tetramer d(GCTA)₂ and the 6F-GTC-d(GCTA)₂ complex at the CG/TA

step using the force field MMX are shown in Figure 2A and 2B respectively. As suggested by the hydrogen bond distances reported in Table 4, the Watson-Crick base pairing was maintained upon intercalation. However, because base pairs must separate vertically to allow intercalation, the sugar-phosphate is destroyed. As seen in Figure 2B, the average separation in the CG/TA base step was increased from 3.5-3.8 Å to 6-8 Å. However, the separation of the other two base steps remained unchanged. The present results showed significant structural changes in the DNA helical structure upon intercalation of GTCs. The results given in Tables 5 and 6 showed that the torsional angles of the phosphate backbone ($\alpha, \beta, \delta, \epsilon, \zeta$ and χ) and sugar ($\nu_1, \nu_2, \nu_3, \nu_4$ and ν_5) change significantly. The definition of these torsion angles is shown in Figure 3. In addition to the observed structural changes in DNA upon intercalation, a small change in the planarity of the GTC molecule has also been observed. For example, the dihedral angles C12C11N10C2, N10C2S1C5 and C2S1C5C6 have been changed from 180° to 175°, 172° and 175° respectively.

Table 3: Binding energies in kcal/mol for 5 and 6 substituted GTC analogues intercalated into DNA tetramer d(GCTA)₂

Substitute	Base step		
	CG/TA	GC/CG	TA/AT
5F	-18.7	9.2	-7.2
5OH	-14.4	3.0	-8.2
5OCH ₂ CH ₃	-12.6	4.5	-3.3
5OCH(CH ₃) ₂	-13.9	-0.9	-2.8
5O(CH ₂) ₃ CH ₃	-20.4	-5.0	-3.7
H	-2.8	4.5	5.5
6F	-12.4	14.7	-8.4
6CH ₃	-17.2	-1.2	-11.6
6CH ₂ CH ₃	-11.4	7.2	-1.4
6OCH ₃	-7.6	-1.6	-3.9
6OCH ₂ CH ₃	-16.6	-0.8	-3.3
6C(CH ₃) ₃	-21.1	-0.6	-14.1
6CH(CH ₃) ₂	-21.1	2.8	3.0

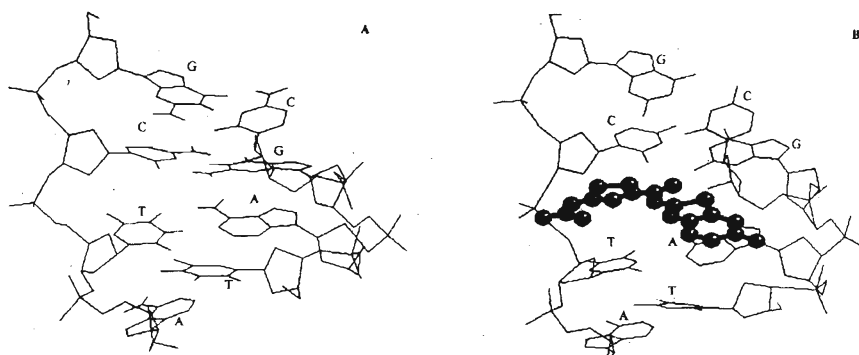


Figure 2: Energy minimised structures using MMX force field. (A) $d(\text{GCTA})_2$ and (B) $6\text{F-GTC-d}(\text{GCTA})_2$ complex. DNA is in wireframe and 6F-GTC is in ball and stick form. Hydrogen atoms are omitted.

Table 4: Hydrogen bond distances of GC and AT base pairs in $d(\text{GCTA})_2$ and 6F-GTC intercalated into $d(\text{GCTA})_2$.

Base pair	H bond ^a	H bond distance/ Å	
		$d(\text{GCTA})_2$	Intercalated $d(\text{GCTA})_2$
GC	$\text{N}_2\text{-O}_2$	3.09	2.84
	$\text{N}_1\text{-N}_3$	3.02	2.81
	$\text{O}_6\text{-N}_4$	2.91	2.85
CG	$\text{N}_2\text{-O}_2$	2.86	2.79
	$\text{N}_1\text{-N}_3$	3.09	2.77
	$\text{O}_6\text{-N}_4$	3.15	2.83
TA	$\text{N}_2\text{-N}_3$	2.90	2.73
	$\text{N}_6\text{-O}_4$	3.13	2.85
	$\text{N}_2\text{-N}_3$	3.17	2.76
	$\text{N}_6\text{-O}_4$	3.28	2.84

^a Atom numbering scheme for GC and AT base pairs is shown in Figure 3

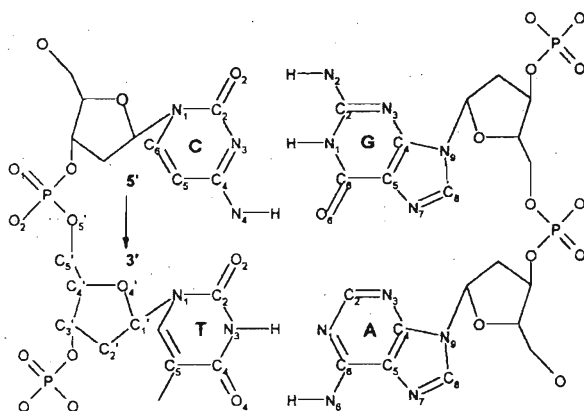


Figure 3: Atomic numbering schemes for DNA base pairs (GC and AT) and phosphate sugar backbone.

Table 5: Phosphate backbone torsion angles in degrees of $d(\text{GCTA})_2$ and 6F-GTC intercalated into $d(\text{GCTA})_2$.

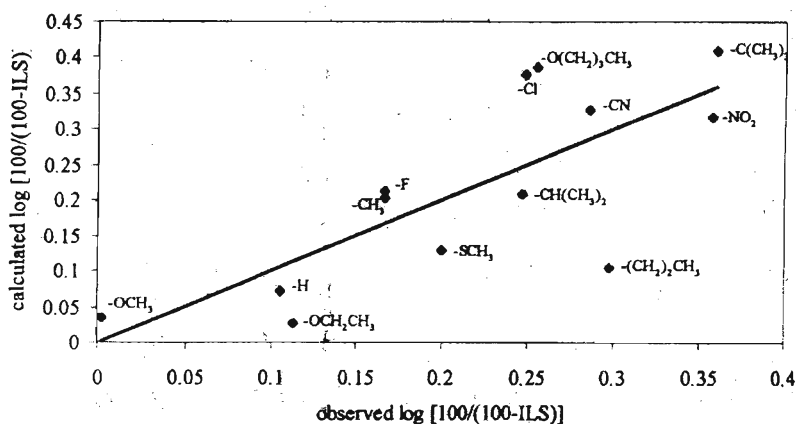
Base step		Torsion angles ^a in degrees						
5'→3'								
	Strand 1	α	β	γ	δ	ϵ	ζ	χ
$d(\text{GCTA})_2$	GC	-78.2	176.5	63.1	93.4	-175.4	-82.9	-138.4
	CT	-68.1	179.8	59.7	162.2	-98.5	169.9	-89.0
	TA	-66.9	158.7	37.6	147.4	-	-	-79.1
Intercalated	GC	-62.6	164.9	61.7	99.4	-153.4	-104.6	138.6
$d(\text{GCTA})_2$	CT	-78.8	-157.3	55.8	126.6	-82.1	154.9	-63.5
	TA	-81.9	12.0	57.2	132.0	-	-	-
Strand 2								
$d(\text{GCTA})_2$	TA	-74.6	146.3	48.6	142.6	-160.4	-110.5	-92.3
	AC	-52.7	146.5	44.9	140.6	-117.1	174.7	-82.6
	GC	-65.0	138.6	48.9	130.8	-108.0	-	-
Intercalated	TA	-69.0	122.8	56.0	127.0	-157.5	-123.0	-75.6
$d(\text{GCTA})_2$	AC	-60.1	175.6	61.6	140.4	-63.7	134.6	-74.5
	GC	-100.1	147.9	56.0	116.1	-134.6	-	-

^a The phosphate backbone torsion angles are defined below using the atom labels and numbering scheme shown in Figure 3. α - $\text{O}_3\text{-P-O}_5\text{-C}_5'$, β - $\text{P-O}_5\text{-C}_5'\text{-C}_4'$, γ - $\text{O}5'\text{-C}_5'\text{-C}_4'\text{-C}_3'$, δ - $\text{C}_5'\text{-C}_4'\text{-C}_3'\text{-O}_3'$, ϵ - $\text{C}_4'\text{-C}_3'\text{-O}_3'\text{-P}$, ζ - $\text{C}_3'\text{-O}_3'\text{-P-O}_5'$, χ - $\text{O}_4'\text{-C}_1'\text{-N}_9\text{-C}_4$ (purines), $\text{O}_4'\text{-C}_1'\text{-N}_1\text{-C}_2$ (pyrimidines)

Table 6: Sugar torsion angles in degrees of d(GCTA)₂ and 6F-GTC intercalated into d(GCTA)₂

Base step 5'→3'		Torsion angles ^a in degrees				
	Strand 1	v ₁	v ₂	v ₃	v ₄	v ₀
d(GCTA) ₂	GC	7.2	10.9	-25.2	30.8	-24.0
	CT	37.0	-38.8	28.2	-5.3	-19.9
	TA	24.3	-33.5	30.5	-15.5	-6.0
Intercalated d(GCTA) ₂	GC	24.6	-2.6	-20.2	37.2	-38.9
	CT	42.4	-27.7	4.5	23.3	-41.4
	TA	41.1	-28.8	8.1	18.4	-37.8
Strand 2						
d(GCTA) ₂	TA	27.5	-32.7	27.2	-10.3	-10.7
	AC	44.6	-36.6	14.8	14.3	-37.8
	GC	39.8	-34.5	16.3	8.9	-30.9
Intercalated d(GCTA) ₂	TA	38.6	-25.4	4.8	20.2	-37.2
	AC	45.5	-35.5	15.6	13.4	-37.5
	GC	37.8	-19.3	-5.1	55.7	-43.1

^a The sugar torsion angles are defined below using the atom labels and numbering scheme shown in Figure 3. v₁ - O₄'-C₁'-C₂'-C₃', v₂ - C₁'-C₂'-C₃'-C₄', v₃ - C₂'-C₃'-C₄'-O₄', v₄ - C₃'-C₄'-O₄'-C₁', v₀ - C₄'-O₄'-C₁'-C₂'

**Figure 4: QSAR correlation using equation 1 with thirteen 6-substituted GTC analogues**

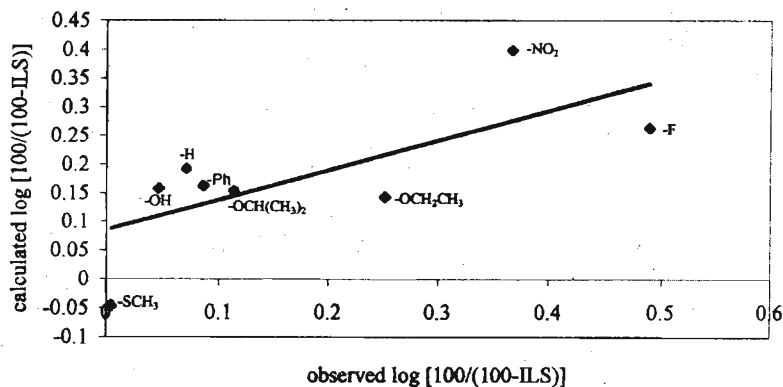


Figure 5: QSAR correlation using equation 2 with eight 5-substituted GTC analogues

Table 7: Calculated and observed efficacy for thirteen 6-substituted GTC analogues

Compound	Substitute	$1/E_{LUMO}$	Log P	$\log [100/(100-ILS)]^{19}$	
				observed ^a	calculated
1	6NO ₂	-0.62907	-0.71	0.3161	0.356437
2	6Cl	-0.83695	0.55	0.3768	0.248189
3	6F	-0.84948	0.15	0.2132	0.166932
4	6CN	-0.75556	0.03	0.3279	0.286374
5	6CH ₃	-0.885	0.48	0.2027	0.166442
6	6C(Me) ₃	-0.88413	1.7	0.4089	0.359266
7	6CH(Me) ₂	-0.91047	1.23	0.208	0.246694
8	6(CH ₂) ₂ Me	-0.88541	1.32	0.105	0.297725
9	6O(CH ₂) ₃	-0.89193	1.11	0.387	0.25515
10	6SCH ₃	-0.85818	0.44	0.128	0.199647
11	H	-0.87501	0	0.0706	0.1058
12	6OCH ₃	-0.93099	-0.13	0.0339	0.002966
13	6OCH ₂ Me	-0.89225	0.21	0.0269	0.113378

^ataken from reference 2

Initially, numerous sets of regression analyses were performed on the singly substituted GTC analogues using theoretically calculated parameters. In all

regression analyses, the probit transformation^{19,20} of biological response (ILS) defined as $\log [100/(100-ILS)]$ has been used as the dependent variable. For example, an analysis using thirteen 6-substituted GTC analogues, see Table 7, resulted in equation (1)

$$\log[100/(100-ILS)] = 1.472(1/E_{LUMO}) + 0.157\log P + 1.394 \dots \dots \dots (1)$$

where 57% of the variance ($R^2=0.57$) in the survival data was accounted for by an equation incorporating the energy of the lowest unoccupied molecular orbital E_{LUMO} and the partition coefficient between octanol and water Log P. Figure 4 shows the correlation graphically of the observed versus calculated $\log [100/(100 - ILS)]^{19}$ values for 6-substituted analogues.

A regression analysis on the set of 5-substituted GTC analogues (Table 8) incorporating $1/E_{HOMO}$ and Log P led to equation 2 that accounted for less of the

$$\log[100/((100-ILS))] = 57(1/E_{HOMO}) + 0.02\log P + 6.65 \dots \dots \dots (2)$$

variance (i.e., $R^2=0.52$) in the observed efficacy data. Figure 5 shows the correlation between the observed and calculated $\log [100/(100-ILS)]^{19}$ values.

Table 8: Calculated and observed efficacy for eight 5-substituted GTC analogues.

Compound Substitute	$1/E_{HOMO}$	Log P	$\log [100/(100-ILS)]^{19}$	
			observed ^a	calculated
1 5F	-0.11201	0.15	0.4895	0.264249
2 5NO ₂	-0.1093	-0.71	0.3665	0.399012
3 5OCHMe ₂	-0.11405	0.43	0.1135	0.154376
4 5Ph	-0.11441	1.67	0.0862	0.162766
5 5OH	-0.11365	-0.39	0.0458	0.158162
6 5SCH ₃	-0.11756	0.44	0.0044	-0.0456
7 5OCH ₂ Me	-0.11416	0.21	0.2518	0.143463
8 H	-0.11322	0	0.0706	0.19187

^a taken from reference 2

DISCUSSION

In the present study, the interaction of GTCs with the double strand DNA sequence d(GCTA)² has been investigated by using the molecular mechanics method. The

results showed that the GTCs intercalate favourably at the CG/TA step of the duplex DNA tetramer. The significant distortions in the double strand structure of the DNA were observed upon intercalation of GTCs. The results also revealed that the planarity of the GTC was also distorted upon the intercalation.

We have demonstrated that the molecular descriptors derived from the quantum chemical and molecular mechanics methods can be used to develop quantitative structure-activity relationships for anti-tumor active GTCs. Two independent QSARs were obtained for 5 and 6 substituted GTC analogues. However, further investigations are required to improve theoretical QSARs obtained in this study and to develop theoretical QSAR for substituted GTC analogues regardless of their substitution position.

Acknowledgement

We would like to thank the National Science Foundation of Sri Lanka for financial support through research grant RG/C/97/01 and the Department of Chemistry, University of Sri Jayewardenepura for computer facilities. We acknowledge the referees of this paper for their valuable comments and suggestions.

References

- 1 Gupta S. P. (1994). Quantitative structure activity relationship studies on anticancer drugs, *Chem. Rev.*, **94**, 1507
- 2 Schnur R. C., Gallaschun R. J., Singleton D. H., Grissom M., Sloan D. E., Goodwin P., McNiff P. A., Fliri A. F., Mangano M., Olson T. M. & Pallack V. A. (1991). Quantitative structure-activity relationships of antitumor guanidinothiazolecarboxyamides with survival enhancement for therapy in the 3LL Lewis lung carcinoma, *J. Med. Chem.*, **34**, 1975
- 3 Schnur R. C., Fliri A. F., Goldfarb R. H. & Pollack V. A. (1991). N-(5-fluorobenzothiazol-2-yl)-2-guanidinothiazole-4-carboxamide, a novel systemically active antitumor agent effective against 3LL Lewis lung carcinoma, *J. Med. Chem.*, **34**, 914
- 4 Braithwaite A. & Baguley B. C. (1980). Existence of an extended series of antitumor compounds which bind to deoxyribonucleic acid by non interactive means, *Biochemistry*, **19**, 1101
- 5 Dervan P. B. (1986). Design of sequence specific DNA binding molecules, *Science*, **232**, 464

- 6 Pullman B. (1989). In: *Advances in Drug Research*, B. Tests, Ed. Academic Press, San Diego, vol 18, pg 1
- 7 Franke R. (1984). *Theoretical drug design methods*, Elsevier, Amsterdam, pp115
- 8 Gupta S. P., Singh S. & Bindal M. C. (1983). QSAR studies on hallucinogens, *Chem. Rev.*, **83**,633
- 9 Gupta S. P. (1987). QSAR studies on enzyme inhibitors, *Chem. Rev.*, **87**, 1183
- 10 Gupta S. P. (1991). Quantitative structure activity relationship studies on local anaesthetics, *Chem. Rev.*, **91**, 1109
- 11 Megee P. S. (1989), ACS Symp. Series, **413**, 37
- 12 Gilbert K. E., Allinger N. L., McKelvey J. & Gajewski J. J., PCMODEL, V6.0, Sarena Software, Box 3076, Bloomington, IN 47402
- 13 Stewart J. P., MOPAC version 5, Frank J. Seiler Research Laboratory, United States Air Force Academy, Colorado Springs, CO 80840
- 14 Hawkins G. D., Giesen D. J., Lynch G. C., Chambers C. C., Rossi I., Storer J. W., Li J., Rinaldi J., Liotard D. A., Cramer C, J. & Truhlar T. G. (1997). AMSOL version 6.5.2. University of Minnesota
- 15 Tereshko R. V., Urpi L., Malinina L., Huynh-Dinh T. & Subirana J., (1996). structure of the B-DNA oligomers d(CGCTAGCC) and d(CGCTCTAGAGCG) in new crystal forms, *Biochemistry*, **35**, 11589
- 16 Ghose A. K. & Crippen G. M. (1987) Calculation of log P values, *J. Chem. Inf. Compu. Sci.*, **21**,27
- 17 Gajewski J. J., Gilbert K. E. & McKelvey J. (1990). MMX: An enhanced version of MM2, in *Advances in Molecular Modeling* vol 2, p 65, Liotta, D. ed Greenwich, Conn, JAI Press, Inc
- 18 CHEMDRAW, Cambridge Software, 100 Cambridge Park Drive, Cambridge, MA 02140
- 19 In reference 2, Schnur et al. carried out analyses on the measurement of biological response (ILS), at a standard dose. They have used a probit transformation [probit = $\log(100/(100 - \text{ILS}))$] as the index of efficacy. According to Schnur *et al.* this probit function provides better discrimination among the

more active compounds and prevents biasing the regression equation with data from a few weakly active analogues.

20. Cramer R. D., in *Advanced Reviews in Medicinal Chemistry* (1976), vol II, p 305, Clarke, F. H. ed., Academic Press, New York